X-692-70-284
PREPRINT

SOLAR WIND INTERACTION WITH MERCURY

N. F. NESS
Y. C. WHANG

JULY 1970

GODDARD SPACE FLIGHT CENTER
GREENBELT, MARYLAND

X692-70-284

Solar Wind Interaction with Mercury

Norman F. Ness*

Laboratory for Space Plasmas
C.N.R. - University of Rome, Rome, Italy

and

Y.C. Whang

Department of Space Science and Applied Physics
The Catholic University of America, Washington, D.C. 20017

July, 1970

(Revised January, 1971)

* On leave from NASA - Goddard Space Flight Center, Greenbelt, Maryland 20771

ABSTRACT

With the exception of its higher density, the planet Mercury is almost equivalent to the moon in many of its physical properties with respect to the solar wind interaction with it. At Mercury's heliocentric distance (0.31 to 0.47 A.U.) the solar wind properties are characterized by a speed ratio $S = 7\text{-}9$, $\beta = 0.3 - 0.5$, $\phi = 155^{\circ} - 165^{\circ}$ and $T_{\parallel}/T_{\perp} = 1.0 - 1.5$. A consideration of the motionally induced magnetic field indicates that Mercury, like the Moon, may reveal information about the conductivity of its interior depending upon whether or not a bow shock exits. In the absence of such a phenomenon, the plasma and magnetic field in the wake region can be studied using the guiding-center approach since the solar wind ion Larmor radius is very small compared to the planetary radius. The prediction of a plasma cavity downwind from the obstacle and associated perturbation of the interplanetary magnetic field in the wake then follows. Decreases of the magnitude of the field occur inside a Mach cone tangential to the planet but outside of the umbral region where a field increase occurs. The axis of the Mercurian Mach cone is aberrated some $6^{\circ} - 11^{\circ}$ from the west of the sun and the Mach angle itself is about $14^{\circ} - 19^{\circ}$. These are about twice those of the lunar wake. Possibly penumbral field increases and stimulated waves upstream and downstream from the wake will also occur.

INTRODUCTION

Among the terrestrial planets, Mercury is the only one for which there is as yet no direct experimental data regarding the characteristics of its behaviour as an obstacle in the supersonic flow of the solar wind. It is the purpose of this paper to review the salient physical properties of the planet and the extrapolated parameters of the magnetized solar wind as they relate to the general problem of the solar wind interaction with Mercury.

There are three possible modes of interaction for the solar wind with the planets and Moon:

1. Strong, associated with the existence of a planetary field and the deflection of the solar wind flow, as in the case of the Earth;
2. Moderate, associated with a sufficiently dense atmosphere and ionosphere or highly conducting interior to effectively deflect the solar wind flow as in the case of Venus and Mars (although the supporting data in the latter case are meager) and
3. Weak, in which the solar wind directly impacts the surface of the obstacle as in the case of the Moon.

See figure 1 for illustrations of these classes; note that the difference between types 1 and 2 is whether it is the planetary field or the ionosphere which is responsible for deflecting the solar wind flow around the planet.

For type 1 and 2 interactions, a detached bow shock wave and a magnetosheath boundary layer develop, with a magnetic tail extending away from the Sun

an appreciable distance for type 1. Whether or not a magnetic tail exists for type 2 is not yet known. For type 3, only a relatively short wake region exists in the anti-solar direction with small perturbations of the interplanetary magnetic field.

The average density of Mercury is approximately 5.4 gms/cm^3 although there is an uncertainty of some 15 percent because of the uncertainty in its radius (2340 km.) and total mass. The planetary orbit is unique in that it has the highest inclination (7°) with respect to the ecliptic, the greatest eccentricity (0.206) and is nearest to the Sun of all the planets (average distance = 0.39 AU). Because of its high eccentricity the perihelion distance is only 0.308 AU while aphelion is 0.467 AU.

Until recently (for example see Glasstone, 1965) it was thought that the rotation period of the planet was synchronous with its sidereal orbital period of 88.0 days, always keeping the same hemisphere facing the Sun. However, a dramatic discovery in planetary radio astronomy (Pettingill and Dyce, 1965) showed that the rotation period is in fact only 59 ± 5 days. A period of 58.7 days is 2/3 of the orbital period and is due to the high eccentricity of the planetary orbit and the mass distribution within the planet (Goldreich and Peale, 1966). The discrepancy with the earlier work, based on optical observations, is an example of the phenomenon of "aliasing" which can occur in discretely sampled time series when not recognized by data interpretaters.

The average density of Mercury is closest to that of the Earth (5.5 gms/cm^3) but its radius and rotation period are nearest to those of the Moon (1738 km

and 29.5 days). Since its average density is high, it appears that the planetary interior may be Earth like and structured with a high density core enclosed by a lower density mantle. The very low rotation rate may not provide the necessary mechanism for the generation of a planetary magnetic field. The absence of any evidence for non-thermal radio emission from the planet is consistent with the absence of a magnetic field containing trapped charged particles like the Earth's radiation belts.

The lack of an intrinsic magnetic field strong enough to deflect the solar wind flow still admits the possibility of a sufficiently dense atmosphere with which a moderate interaction can occur. However, in light of the study by Belton et al. (1967) it appears doubtful that an appreciable atmosphere exists with a surface pressure exceeding 10^{-3} millibars. The optical properties of the top surface layer of Mercury are very close to those of the Moon, as is its albedo (Mercury = 0.06, Moon = 0.07) (Dollfus, 1961; Murdock and Ney, 1970). Thus, with the exception of its anomalously high density, Mercury is almost equivalent to the Moon in many of its intrinsic physical properties. The possibility of a conducting interior is treated in section 3.

The possibility of an interaction with a very rarified atmosphere has recently been discussed by Banks et al. (1970). They conclude that there is a reasonable possibility for a sufficiently well developed ionosphere such that the solar wind will be deflected. Such an effect can take place for atmospheres whose surface pressures are considerably less than 10^{-3} mb. When the solar wind is

deflected, a detached bow shock is formed in the upstream of the planet similar to the solar wind interaction with the conducting planetary ionosphere (Elco, 1969; Cloutier et al. 1969) or the gaseous envelope of a comet (Biermann et al. 1967). In the remainder of this paper it will be assumed that the interaction is similar to that with the moon since the alternate case has recently been discussed by Banks et al. (1970).

SOLAR WIND PROPERTIES

In the past decade, the properties of the solar wind have been established from direct observations between 0.7 and 1.5 AU by various spacecrafts. The observed quiet state of the solar wind (Hundhausen, 1970) at 1 AU has a speed $V = 320$ km/sec, proton density $n = 8$ cm^{-3}, electron temperature $T_e = 1.5 \times 10^5$ °K, and proton temperature $T_p = 4 \times 10^4$ °K. The relationship between the proton temperature and flow speed of the observed solar wind is characterized by an empirical relation (Burlaga and Ogilvie, 1970).

$$\sqrt{T_p} = 0.036\, V - 5.54 , \qquad (1)$$

for V between 250 and 750 km/sec, where T_p is in units of 10^3 °K and V in km/sec. The electron temperature appears to be nearly independent of V and varies much less than the proton temperature (Montgomery et al., 1968). The measured interplanetary magnetic field at 1 AU has an average magnitude of 6 γ and an average direction angle $\phi = 135^\circ$ or 315° (Ness, 1968). The thermal motion of the solar wind plasma is anisotropic (Hundhausen et al., 1967), for protons the average $T_{\parallel}/T_{\perp}$ is about 1.5 while for electrons the temperature anisotropy is usually less than 1.2.

Since the original application of the hydrodynamic equations to the solar wind problem by Parker (1958), a number of theoretical models have been developed to study the solar wind, notably the one-fluid models studied by Noble and Scarf (1963) and by Whang and Chang (1965), and the two-fluid

model by Sturrock and Hartle (1966) and by Hartle and Sturrock (1968). The results predicted by the one-fluid model give reasonable agreement (Hundhausen, 1970) with the observed velocity and density of the quiet solar wind at 1 AU. The predicted temperature is close to the observed electron temperature, but it is about four times the observed proton temperature.

The results predicted by the two-fluid model are in agreement with the extrapolated T_p, V-relation of Burlaga and Ogilvie (1970). However, the two-fluid model is in disagreement with the observations of the fraction of the total energy flux carried by heat conduction at 1 AU. The one-fluid model of Whang and Chang (1965) predicted a heat conduction flux close to that actually observed (Hundhausen, 1969).

The nature of the interaction of the solar wind with a planetary body is determined by two factors: (i) the solar wind conditions upstream from the obstacle presented by the planetary body, and (ii) the properties of the planetary body which determines how the obstacle responds to the impinging interplanetary plasma and field lines. The steady-state solar wind conditions at the orbits of different planets can be characterized by

1. a dimensionless velocity parameter which can be represented by the ratio of the solar wind speed to a characteristic speed of the plasma, such as the Mach number, the Alfven number or the speed ratio.
2. the ß-value of the plasma,

3. the direction angle of the interplanetary field, ϕ , and

4. the temperature anisotropy, $T_{\parallel}/T_{\perp}$.

These parameters are listed in descending order of importance at 1 AU with respect to the solar wind interaction with the Moon (see review by Ness, 1970). Near the earth's orbit, the speed ratio

$$S = V(\rho/P_{\parallel})^{1/2} \sim 11 ,$$

and the ß-value is ~ 1.

Assuming that the radial dependence of the solar wind properties predicted by the one-fluid model of Whang and Chang (1965) is appropriate, we can extrapolate the solar wind properties to the orbits of other planets, based on the observed solar wind properties at 1 AU and the spiral model of the interplanetary magnetic field (Parker, 1958).

From the extrapolated solar wind properties, one can estimate that throughout Mercury's orbital range of heliocentric distance

$S = 7\text{-}9$

$ß = 0.3 - 0.5$

and $\phi = 155^{\circ} - 165^{\circ}$ $(335^{\circ} - 345^{\circ})$

The average temperature anisotropy at Mercury's orbit must be between 1 and 1.5. Because the proton temperature predicted by the one-fluid model is

about three times the observed proton temperature, probably the proton temperature decreases faster as a function of the heliocentric distance than that predicted by the one-fluid model. Taking this effect into consideration, at Mercury's orbit the ß-value would be slightly larger and the speed ratio S slightly less than predicted.

MOTIONALLY INDUCED MAGNETIC FIELD

As the solar wind convectively transports the imbedded interplanetary magnetic field past a planet, there is an apparent electrical field, $E = -V \times B$, which is observed in a frame of reference fixed to the planet. This motionally induced electrical field is due to the high conductivity of the solar wind plasma which requires that $(\underline{E} + \underline{V} \times \underline{B}) \rightarrow 0$ in the plasma. If the coupling between the conducting interior of the planet and the plasma through the planetary surface and plasma sheath layer is sufficiently good, then an electrical current will flow through the body of the planet and generate a secondary magnetic field. This mechanism has been studied in the case of the Moon and planets by Sonett and Colburn (1968) and the Moon by Hollweg (1968), Dessier (1968) also suggested that the same mechanism might be active for the planet Mars with only the planetary ionosphere participating in the role of the conducting body.

If the conductivity is sufficiently high, the secondary magnetic field, a dipolar field, will be strong enough to deflect the solar wind flow and hence lead to the formation of a shock wave and a plasma sheath layer. A planet whose internal temperature is higher than its surface may be considered as a low conductivity surface layer (σ_s) surrounding a higher conductivity core (σ_c). From Hollweg (1968) we may derive an approximate relationship for the critical conductivity of the surface layer leading to the formation of a shock as a function of the interplanetary magnetic field parameters B and ϕ and the internal structure of the

MOTIONALLY INDUCED MAGNETIC FIELD

As the solar wind convectively transports the imbedded interplanetary magnetic field past a planet, there is an apparent electrical field, $E = -V \times B$, which is observed in a frame of reference fixed to the planet. This motionally induced electrical field is due to the high conductivity of the solar wind plasma which requires that $(\underline{E} + \underline{V} \times \underline{B}) \rightarrow 0$ in the plasma. If the coupling between the conducting interior of the planet and the plasma through the planetary surface and plasma sheath layer is sufficiently good, then an electrical current will flow through the body of the planet and generate a secondary magnetic field. This mechanism has been studied in the case of the Moon and planets by Sonett and Colburn (1968) and the Moon by Hollweg (1968), Dessier (1968) also suggested that the same mechanism might be active for the planet Mars with only the planetary ionosphere participating in the role of the conducting body.

If the conductivity is sufficiently high, the secondary magnetic field, a dipolar field, will be strong enough to deflect the solar wind flow and hence lead to the formation of a shock wave and a plasma sheath layer. A planet whose internal temperature is higher than its surface may be considered as a low conductivity surface layer (σ_s) surrounding a higher conductivity core (σ_c). From Hollweg (1968) we may derive an approximate relationship for the critical conductivity of the surface layer leading to the formation of a shock as a function of the interplanetary magnetic field parameters B and ϕ and the internal structure of the

planet.

Let $X = R_c / R_m$ be the normalized size of the core, the ratio of the core radius to the radius of the planet, and the conductivity contrast $= \sigma_c / \sigma_s$. On the planetary surface, the pressure due to the induced magnetic field is

$$\frac{B_i^2}{2\mu} = \frac{\mu}{8} \left(R_m \sigma_s f V B \sin\phi \sin\theta \right)^2 \qquad (2)$$

where Θ is the colatitude measured from the axis defined by the direction of the motional electric field $\underline{E}_m$ $(= - \underline{V} \times \underline{B})$, and f is a function given by

$$f = \frac{2 (1 - X^3) + (\sigma_c / \sigma_s) (1 + 2 X^3)}{2 + X^3 + (\sigma_c / \sigma_s) (1 - X^3)} \qquad (3)$$

The normal component of the pressure due to the solar wind flow is

$$p = K m_p n (V \sin\theta \cos\omega)^2 \qquad (4)$$

where ω is the longitude measured from the meridian plane defined by the two vectors $\underline{V}$ and $\underline{E}_m$, and m_p the proton mass. From equations (2) and (4) we can obtain the critical surface conductivity

$$\sigma_s = \frac{\sqrt{8 K m_p n / \mu} \cos\omega}{B R_m f \sin\phi} \qquad (5)$$

The critical conductivity is independent of the solar wind velocity V and the colatitude θ. This is because the induced magnetic pressure and the solar wind pressure normal to the surface are both directly proportional to $V^2 \sin^2\theta$.

For a uniformly conducting interior ($\sigma_s = \sigma_c$), on the meridian plane ($\omega = 0$) the critical conductivity is found to be 3.2×10^{-5} mhos/meter for $B \sin\phi = 10\,\gamma$ and $n = 60\ cm^{-3}$. This is only slightly less than the critical conductivity for the moon

(4.2×10^{-5} mhos/meter). The variation of σ_s versus σ_c for both the Moon and Mercury on the meridian plane defined by the vectors $\underset{\sim}{V}$ and $\underset{\sim}{E}_m$ is shown in figure 2 for values of X ranging from 0.4 to 0.99. It is seen that for normalized core sizes less than 0.4, there is essentially no effect on the critical conductivity regardless of the core conductivity. Also note that from this induced field consideration, the Moon and Mercury are very much alike.

The electrical conductivity of typical rock materials in the interior of a planet is determined by composition, pressure and temperature, being a very sensitive function of the latter parameter. It increases enormously as the temperature increases only slightly. For the near surface material, the conductivity is dependent principally upon the conductivity of the fluids which fill the cracks and interstices. Nothing is known of the thermal state of the interior of Mercury although it is certain that the temperature must be higher in the core due to the presence of radioactive elements and the low thermal diffusivity of ordinary silicate rocks. The surface temperatures ($\sim 600^{\circ}$ K) appear to be consistent with a black body in equilibrium with its surroundings. The absence of an appreciable atmosphere and the modest temperatures of the surface argue against a high electrical conductivity surface layer. Note that the critical conductivity decreases rapidly as the core conductivity increases above the critical value.

At present it appears doubtful that the conductivity of the surface layer is sufficiently high to lead to the development of a strong enough

secondary magnetic field to deflect the solar wind flow. However, the high average density of the planet indicates probably the existence of a core, whose conductivity might be high enough, as well as being large enough to compensate for the low conductivity surface layer . Under these conditions, then a moderate interaction of the solar wind would occur. In the following section it will be assumed that the effective conductivity of the planet is less than that required to form a bow shock and that the interaction of the solar wind will in fact be Moon-like.

MOON-LIKE INTERACTION

If the internal electrical properties of Mercury are similar to those of the moon, then the solar wind plasma impinging on Mercury is fully absorbed by its surface and the interaction of the solar wind is expected to be quite similar to that with the Moon.

Research work on the interaction of the solar wind with the moon has recently been summarized by Ness (1970). Theoretical studies of the solar wind-moon interaction have been carried out using two approaches: the continuum fluid approach (Johnson and Midgley, 1968; Michel, 1968; Spreiter et al., 1970; and others) and the guiding-center plasma approach (Whang, 1969).

The guiding-center model provides a quantitative basis for predicting the characteristics of the solar wind-Mercury interaction. The guiding-center approximation to study the interaction of the solar wind with a planetary body is valid when the Larmor radius of the solar wind protons is very small compared with the radius of the planetary body. The proton Larmor radius at the Mercurian orbit is less than 10 km, while the radius of the planet Mercury is about 1.4 times that of the Moon. This means that the guiding-center approximation should work for Mercury even better than for the Moon.

The interaction of the solar wind with Mercury is expected to form a plasma cavity like the one observed behind the moon (Lyon, et al. 1967).

Using the guiding-center model of Whang (1969), one can calculate the two-dimensional solution for the perturbations of the magnetic field on the plane of symmetry (defined by the two vectors $\underline{V}$ and $\underline{B}$) behind Mercury. Assuming that the magnetic field increases slightly near the lunar limbs and that $S = 8$, $\beta = 0.5$, $\phi = 160^{\circ}$ and $T_{\parallel} / T_{\perp} = 1.5$ as appropriate at the orbit of Mercury, a numerical solution is calculated as shown in figure 3. The principal perturbations of the field (the umbral increase and the penumbral decrease) are confined to a region bounded by a Mach cone tangential to Mercury like the observed lunar Mach cone (Whang and Ness, 1970). Because the field direction angle $\phi \sim 160^{\circ}$ (or 340°), the Mach angle of the cone is nominally very close to $\alpha_{\perp}$, corresponding to the perpendicular propagation of magnetoacoustic waves. The speed ratio of the solar wind at Mercury's orbit $S \sim 8$, thus from figure 4 it is seen that the Mach cone in the Mercurian wake should have a Mach angle of approximately 15° which is about 2-3 times the Mach angle in the lunar wake.

In the case of the Moon, positive perturbations of the interplanetary magnetic field are sometimes observed just outside the Mach cone. They represent the propagation of field increases near the lunar limb to the downstream. There is as yet no satisfactory explanation for the occurrence of the field increase near the lunar limbs (see review by Ness, 1970) and so it is not possible to predict definitely their presence or absence for Mercury. In addition, stimulated waves from the lunar wake may have their counterpart in the Mercurian environment (Ness and Schatten, 1970).

The orbital velocity of Mercury ranges from 35 to 59 km./sec. Thus the aberrated direction of the solar wind flow from West of the Sun nominally ranges from 7° to 11°. The natural variations in the solar wind velocity may alter this by $\pm 10^{\circ}$. Hence, the axis of the interaction region aftward of Mercury will be deviated from the anti-solar direction by an angle twice that of the Earth (Behannon, 1970) or the Moon (Whang and Ness, 1970).

SUMMARY

The properties of the planet Mercury and the solar wind at the orbit of Mercury are such that it is expected that the solar wind-planet interaction may be quite moon-like in its characteristics. This means the existence of a plasma cavity behind the planet with an increased interplanetary magnetic field magnitude in the umbra and associated penumbral decreases. Possibly penumbral increases and stimulated waves upstream from the wake will also occur. The principle differences are a slight modification of the wake geometry, with the axis aberrated some 6° to 11° and the Mach-cone angle being 14° to 19°. These are about twice those in the case of the Moon.

If a bow shock exists surrounding the planet, then it indicates a rather higher electrical conductivity for the Mercurian interior than for the Moon, or the presence of an atmosphere sufficiently dense to deflect the solar wind flow. This later situation has recently been treated by Banks et al. (1970). In this case the characteristics of the interaction will be like that at Mars.

ACKNOWLEDGMENTS

We appreciate discussions of this work with Mr. K.W. Behannon and Drs. L.F. Burlaga, K.W. Ogilvie and K.H. Schatten. The work at the Catholic University of America was supported by the National Aeronautics and Space Administration under Grant NGR-09-005-063.

REFERENCES

Banks, P.M., H.E. Johnson and W.I. Axford, The atmosphere of Mercury, to be published, 1970.

Belton, M.J.S., D.M. Hunten and M.B. McElroy, A search for an atmosphere on Mercury, Astrophys. J., 150, 1111, 1967.

Behannon, K.W., Geometry of the geomagnetic tail, J. Geophys. Res., 75, 743, 1970.

Biermann, L., B. Brosowski, and H.U. Schmidt, The interaction of the solar wind with a comet, Solar Phys., 1, 254, 1967.

Burlaga, L.F. and K.W. Ogilvie, Heating of the solar wind, Astrophys. J., 159, 659, 1970.

Cloutier, P.A., M.B. McElroy, and F.C. Michel, Modification of the Martian ionosphere by the solar wind, J. Geophys. Res., 74, 6215, 1969.

Dessler, A.J., Ionizing plasma flux in the Martian upper atmosphere, in the Atmospheres of Venus and Mars, edited by J.C. Brandt and M.B. McElroy, pg. 241, Gordon and Breach, N.Y., 1968.

Dollfus, A. in Planets and Satellites, ed. by G.P. Kuiper and B.M. Middlehurst, chapter IX. Univ. of Chicago, Chicago, 1961.

Elco, R.A., Interaction of the solar wind with planetary atmosphere, J. Geophys. Res., 74, 5073, 1969.

Glasstone, S. Source book on the Space Sciences, Chap. X, D. Van Nostrand Co. Inc., Princeton, N.J., 1965.

Goldreich, P. and S.J. Peale, Resonant spin states in the solar system, Nature 209, 1078, 1966.

Hartle, R.E. and P.A. Sturrock, Two fluid model of the solar wind, Astrophys. J., 151, 1155, 1968.

Hollweg, J.H., Interaction of the solar wind with the Moon and formation of a lunar limb shock wave, J. Geophys. Res., 73, 7269, 1968.

Hundhausen, A.J., Bame, S.J., and Ness, N.F., Solar wind thermal anisotropies: Vela 3 and IMP 3, J. Geophys. Res., 72, 5265, 1967.

Hundhausen, A.J., Composition and dynamics of the solar wind plasma, Rev. Geophys. Space Sci., 8, 729, 1970.

Hundhausen, A.J., Nonthermal heating in the quiet solar wind, J. Geophys. Res. 74, 5810, 1969.

Johnson, F.S. and J.E. Midgeley, Notes on the lunar magnetosphere, J. Geophys. Res., 73, 1523, 1968.

Lyon, E.F., H.S. Bridge, and J.H. Binsack, Explorer 35 plasma measurements in the vicinity of the moon, J. Geophys. Res., 72, 6113, 1967.

Michel, F.C., Magnetic field structure behind the moon, J. Geophys. Res., 72, 1533, 1968.

Montgomery, M.D., S.J. Bame and A.J. Hundhausen, Solar wind electrons: Vela 4 measurements, J. Geophys. Res., 73, 4999, 1968.

Murdock, T.L. and E.P. Ney, Mercury: the dark-side temperature, Science, 170, 535, 1970.

Ness, N.F., Observed properties of the interplanetary plasma, Annual Rev. of Astronomy and Astrophys. 6, 79, 1968.

Ness, N.F., Interaction of the solar wind with the moon, NASA-GSFC preprint X-692-70-141, 1970.

Ness, N.F. and K.W. Schatten, Detection of the interplanetary magnetic field fluctuations stimulated by the lunar wake, J. Geophys. Res., 74, 6425 (1969).

Noble, L.M. and F.L. Scarf, Conductive heating of the solar wind, 1, Astrophys. J., 138, 1169, 1963.

Parker, E.N., Dynamics of the interplanetary gas and magnetic fields, Astrophys. J. 128, 664, 1958.

Pettingill, G.H. and R.B. Dyce, A radar determination of the rotation of the planet Mercury, Nature, 206, 1240, 1965.

Sonett, C.P. and D.S. Colburn, The Principle of solar wind induced planetary dynamos , Phys. Earth Planet. Interiors, 1, 326, 1968.

Spreiter, J.R., M.C. March, and A.L. Summer, Hydromagnetic aspects of solar wind flow past the moon, Cosmic Electrodynamics 1, 5, 1970.

Sturrock, P.A. and R.E. Hartle, Two-fluid model of the solar wind, Phys. Rev. Letters, 16, 628, 1966.

Whang, Y.C., and C.C. Chang, An inviscid model of the solar wind, J. Geophys. Res., 70, 4175, 1965.

Whang, Y.C., Field and plasma in the lunar wake, Phys. Res., 186, 143, 1969.

Whang, Y.C., and N.F. Ness, Observations and interpretation of the lunar Mach cone, J. Geophys. Res., 75, 6002, 1970.

FIGURE CAPTIONS

Figure 1 Types of solar wind-planetary body interactions, classified according to amount of deflection of flow and development of features characteristic of supersonic flow past the obstacle.

Figure 2 Variation of critical conductivity of the surface layer (σ_s) as function of core conductivity (σ_c) for nominal solar wind parameters which determine whether or not there may exist a shock wave sustained by secondary magnetic fields generated by a motionally induced electrical current flow.

Figure 3 A two-dimensional solution for perturbations of the magnetic field on the plane of symmetry (defined by the two vectors $\underline{V}$ and $\underline{B}$) behind Mercury. Units of distance are Mercurian Radii and magnitude perturbations are scaled as indicated.

Figure 4 The Mach angles as a function of the speed ratio S and the ß-value. Here $\alpha_\perp$ is the Mach angle corresponding to the perpendicular propagation speed of magnetoacoustic waves, and $\alpha_\parallel$ to the parallel propagation speed.

FIGURE CAPTIONS

Figure 1 Types of solar wind-planetary body interactions, classified according to amount of deflection of flow and development of features characteristic of supersonic flow past the obstacle.

Figure 2 Variation of critical conductivity of the surface layer (σ_s) as function of core conductivity (σ_c) for nominal solar wind parameters which determine whether or not there may exist a shock wave sustained by secondary magnetic fields generated by a motionally induced electrical current flow.

Figure 3 A two-dimensional solution for perturbations of the magnetic field on the plane of symmetry (defined by the two vectors $\underline{V}$ and $\underline{B}$) behind Mercury. Units of distance are Mercurian Radii and magnitude perturbations are scaled as indicated.

Figure 4 The Mach angles as a function of the speed ratio S and the ß-value. Here $\alpha_\perp$ is the Mach angle corresponding to the perpendicular propagation speed of magnetoacoustic waves, and $\alpha_\parallel$ to the parallel propagation speed.

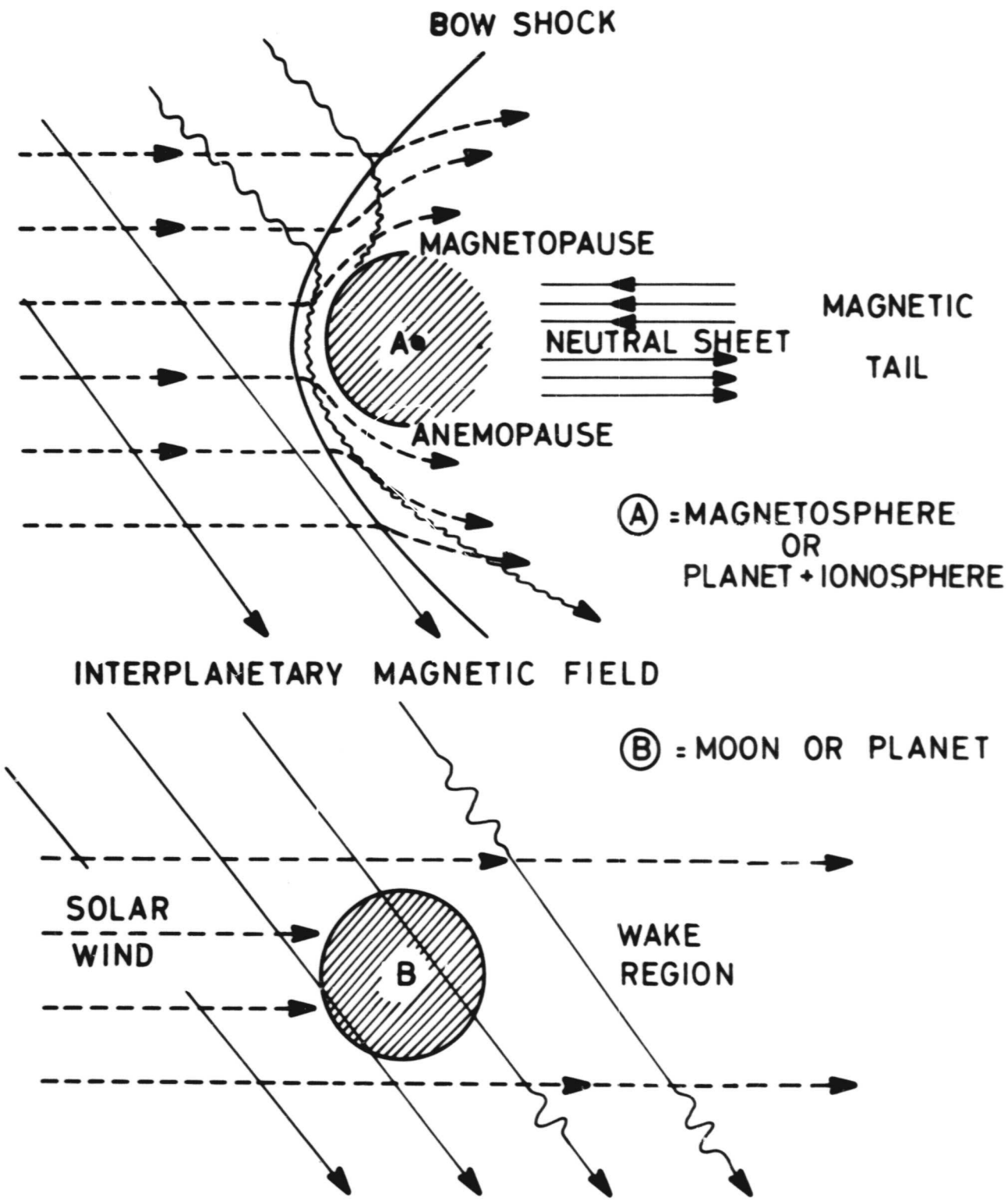

INTERACTION:

STRONG

MODERATE

WEAK

FIGURE 1

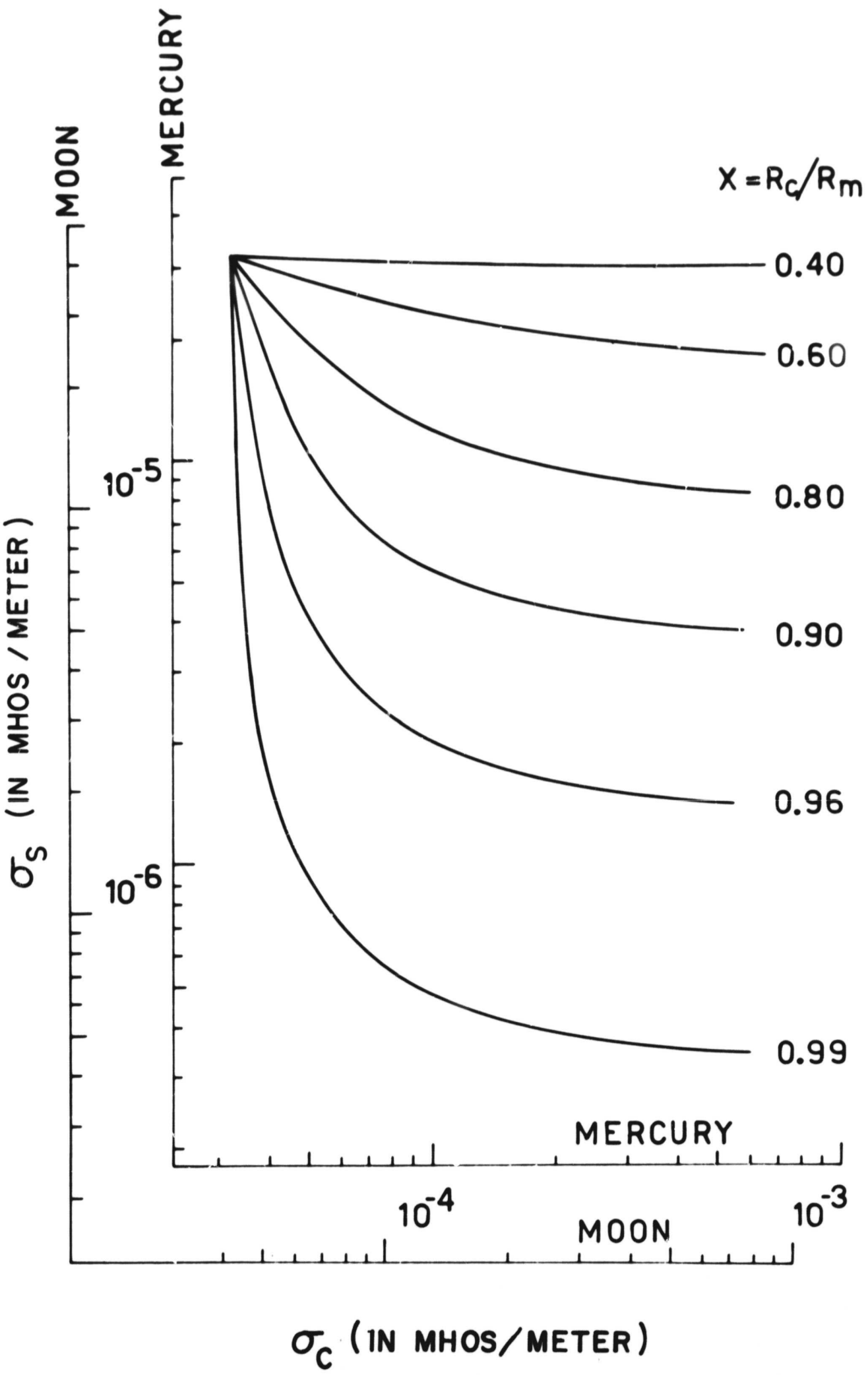
MERCURY
MOON
10^{-5}
10^{-6}
σ_s (IN MHOS / METER)
$X = R_c/R_m$
0.40
0.60
0.80
0.90
0.96
0.99
MERCURY
10^{-4}
MOON
10^{-3}
σ_c (IN MHOS/METER)

FIGURE 2

$$S = 8\ ,\ \beta = 0.5,\ \phi_0 = 160^\circ\ ,\ \frac{T_{11\,0}}{T_{\perp\,0}} = 1.5\ ,$$

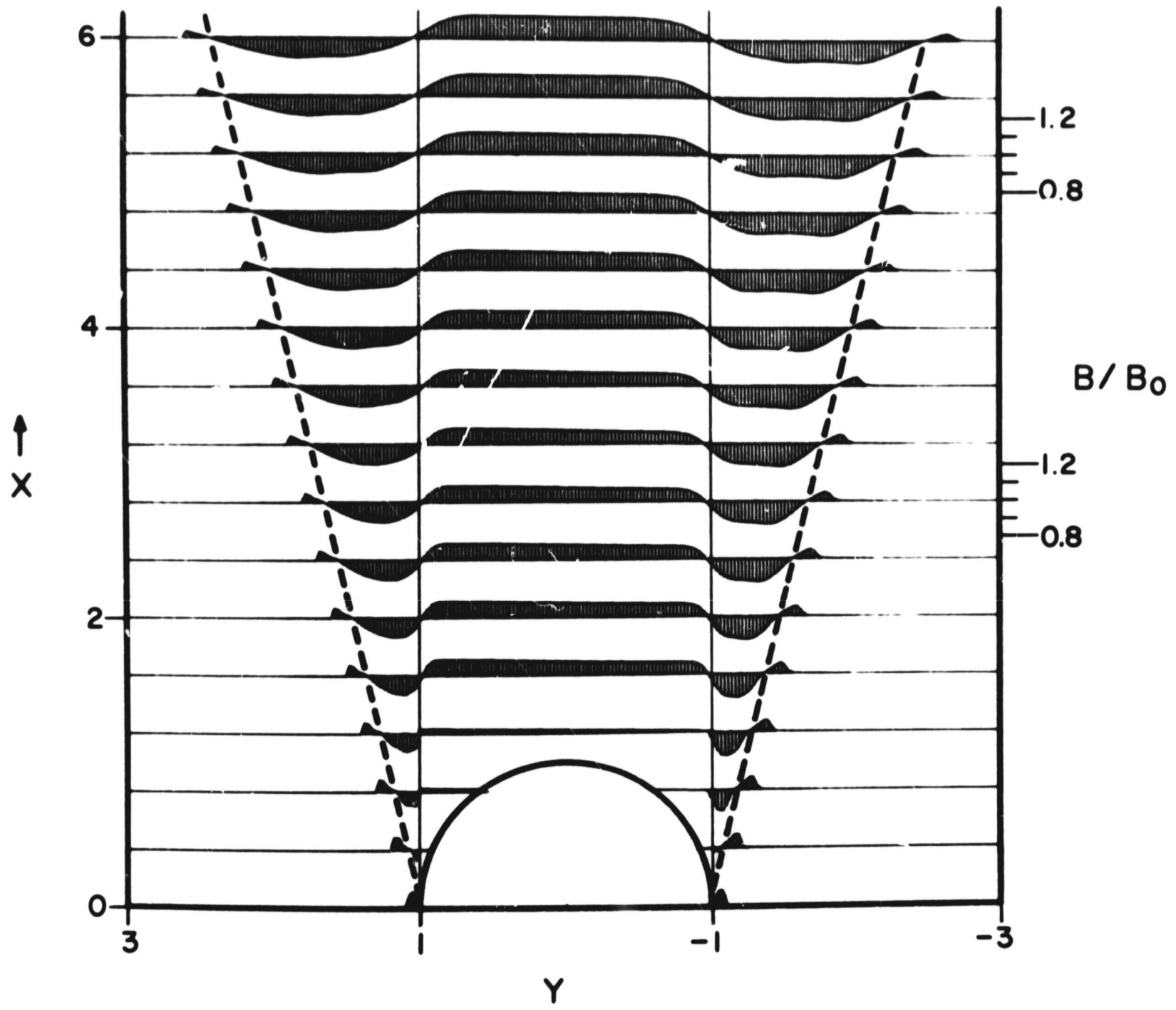

FIGURE 3

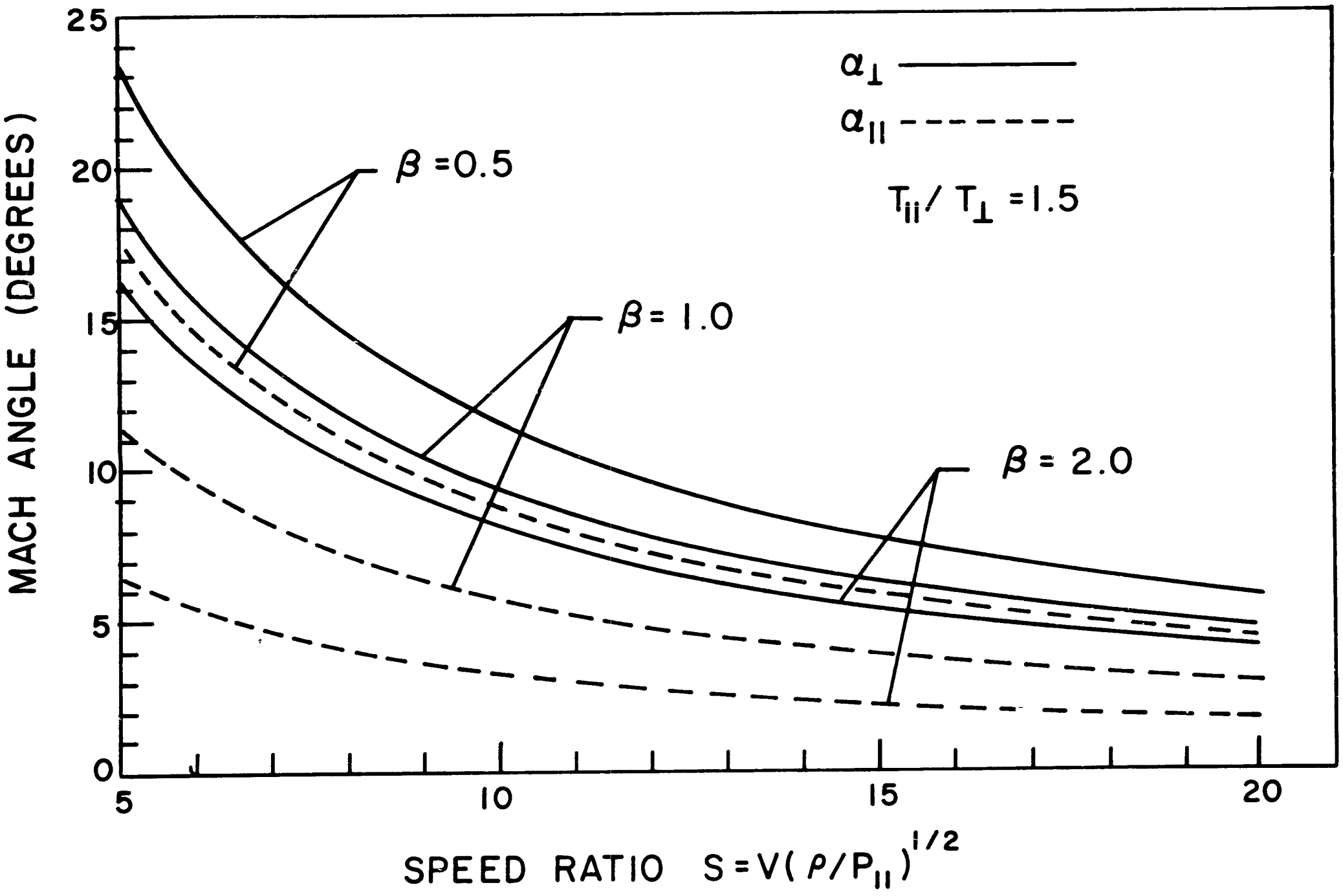
MACH ANGLE (DEGREES)
25
20
15
10
5
0
5
10
15
20
SPEED RATIO S = V(ρ/P11)^1/2
α⊥
α||
T||/ T⊥ =1.5
β =0.5
β= 1.0
β = 2.0

FIGURE 4